minerals

MDPI

Article

Evaluation of Binderless Briquettes as Potential Feed for the Electric Arc Furnaces at Barro Alto, Brazil

Johnny Obakeng Mogalanyane [1], Natasia Naudé [2] and Andrie Mariana Garbers-Craig [1,*]

[1] Centre for Pyrometallurgy, Department of Materials Science & Metallurgical Engineering, University of Pretoria, Private Bag X20, Hatfield, Pretoria 0028, South Africa; johnny.mogalanyane@coremet.co.za
[2] Minerals Processing, Department of Materials Science & Metallurgical Engineering, University of Pretoria, Private Bag X20, Hatfield, Pretoria 0028, South Africa; natasia.naude@up.ac.za
* Correspondence: andrie.garbers-craig@up.ac.za

Abstract

Barro Alto processes nickel laterite ore using rotary kilns and six-in-line rectangular electric arc furnaces. This study evaluated the briquetting of ferronickel ore to reduce kiln fines, improve furnace charge permeability, and enhance process safety. Binderless briquettes were produced from screened ore at two size fractions (−6.3 mm and −12.5 mm), with moisture contents of 16% and 24%, cured under closed and open conditions. The physical and metallurgical properties of the briquettes were assessed using ISO standard tests. The results confirmed successful agglomeration of the ore into binderless briquettes. Screening the run-of-mine (ROM) ore improved the feed quality, increasing the NiO grade from 2.0% to 2.2% in the −6.3 mm fraction. The briquettes from the −6.3 mm ore at 16% moisture exhibited the highest green strength (559 N). Higher moisture content reduced the briquette strength and increased both the reduction disintegration and decrepitation indices. The decrepitation index increased from 0.33% to 0.61% for the −6.3 mm briquettes when the moisture increased from 16% to 24%. The reduction levels were 33.4% and 39.2% for −6.3 mm and −12.5 mm briquettes with 16% moisture, respectively. This study concludes that optimal performance was achieved using −6.3 mm ore, 16% moisture, and open curing, thereby balancing reduction efficiency and mechanical stability.

Keywords: ferronickel briquettes; particle size distribution; moisture content; curing conditions; properties

Academic Editor: Kenneth N. Han

Received: 6 June 2025
Revised: 9 July 2025
Accepted: 16 July 2025
Published: 19 July 2025

Citation: Mogalanyane, J.O.; Naudé, N.; Garbers-Craig, A.M. Evaluation of Binderless Briquettes as Potential Feed for the Electric Arc Furnaces at Barro Alto, Brazil. *Minerals* **2025**, *15*, 756. https://doi.org/10.3390/min15070756

1. Introduction

The Barro Alto deposit is a nickel laterite ore body that consists of three main ore types that occur in six different areas in the State of Goiás in Brazil [1]. These ore types are classified into three categories based on their nickel and iron contents and SiO_2/MgO mass ratios: Plain-Type Ore (1.3 mass% Ni, 21 mass% Fe, SiO_2/MgO mass ratio of 1.7), East-Type Ore (1.6 mass% Ni, 15 mass% Fe, SiO_2/MgO mass ratio of 1.6), and West-Type Ore (1.8 mass% Ni, 19 mass% Fe, SiO_2/MgO mass ratio of 3.1) [2]. The Barro Alto mine, which is wholly owned and operated by Anglo American, is in the Barro Alto complex, which stretches over a 35 km arc from the southwest to the northeast. Its main mineral resource consists of saprolite covered by laterites, containing serpentinised dunites and pyroxenes [3]. Ratié et al. (2018) investigated the nickel distribution in samples from the Barro Alto complex, confirming the presence of serpentine ($(Mg,Fe,Ni,Al,Zn,Mn)_{2-3}(Si,Al,Fe)_2O_5(OH)_4$), magnetite ($Fe_3O_4$), quartz ($SiO_2$), chlorite

($(Mg,Fe)_3(Si,Al)_4O_{10}(OH)_2.(Mg,Fe)_3(OH)_6$), goethite (Fe(OH)O), talc ($Mg_3Si_4O_{10}(OH)_2$), and smectite ($(Na,Ca)_{0.33}(Al,Mg)_2Si_4O_{10}(OH)_2(H_2O)_n$) [2].

With approximately 60% of the world's nickel resources in laterites [4], these ores are poised to be a major nickel source due to lower operational costs compared to sulphide deposits, higher grades, lower mining expenses, and stricter sulphur dioxide emission regulations favouring laterite nickel production [5]. The Barro Alto plant employs a rotary kiln–electric arc furnace route to process ore, with two 185 m rotary kilns and two six-in-line rectangular electrical furnaces (Figure 1). The process begins with size reduction using a sequence of primary, secondary, and tertiary crushers. The crushed material is stockpiled to create a constant feed to the plant and to homogenise the feed material. A reclaimer is used to feed the material into a dryer. The drying takes place in a rotating dewatering kiln, which reduces the moisture content to approximately 22%, depending on the operation. The dried material is screened for top-size control prior to stockpiling. The dewatered ore is then fed to the upper end of the rotary kiln with coal and recycled pelletised dust from the calcination kiln. The combined material is processed through calcination kilns to remove any excess moisture, producing a completely dry and partially reduced ore. Nickel- and iron- containing oxides are reduced in electric arc furnaces and collected as an alloy, while MgO, SiO_2, and Al_2O_3 are collected in the slag.

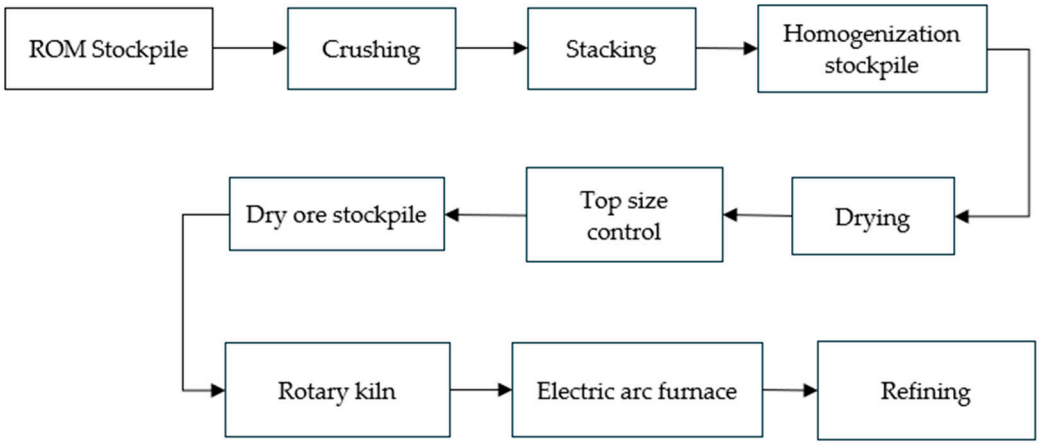

Figure 1. Barro Alto plant block flow diagram [1].

The use of fines without prior agglomeration in an electric arc furnace harms furnace performance, causing lower productivity, reduced charge permeability, and decreased metal extraction. The accumulation of fines from ferroalloy processing and the decline in high-grade ores have been the key drives for the need to agglomerate ores prior to processing [6].

The current study focusses on briquetting as an alternative method for agglomerating nickel laterite ore from the Barro Alto mine in Brazil. The Anglo American Barro Alto industrial complex prioritises sustainability, aiming to cut carbon dioxide (CO_2) emissions from its thermal operations [7].

In 2021, Vale initiated load tests on its iron briquette plant at the Tubarão Unit in Brazil [8]. According to Vale, the adoption of briquettes could lead to a substantial reduction in greenhouse gas emissions, potentially up to 10%, compared to the traditional blast furnace process. This reduction is attributed to the elimination of the carbon-intensive sintering stage.

Additionally, Vale stated that the use of briquettes reduces emissions of particulates and harmful gases, such as sulphur dioxide (SOx) and nitrogen oxides (NOx), as well as the need for water in the production process [8]. With Anglo American's target to reduce

greenhouse gas emissions by 30% by 2030 [9], the use of briquettes could play a crucial role in reaching this goal, given the findings from Vale's research.

In this context, the current study derives its relevance from operational, financial, and environmental sustainability considerations. This study aimed to evaluate the impact of particle size distribution, moisture content, and curing conditions on the performance of binderless briquettes, ultimately identifying the optimum conditions for briquette production and performance.

2. Background

2.1. Briquetting

Briquetting, a method of agglomerating fines from steel and iron production, dates back to the 19th century. Finland saw the first successful industrial application in 1989, agglomerating fine magnetite ore without binders and consuming 5 kWh per ton of briquettes [10]. The slow development of briquetting technology has made methods like sintering and pelletisation more favourable. Findings by Vining et al. (2017) show that briquettes can be produced without grinding, offering energy savings and higher productivity compared to pellets [11]. Preliminary studies by Anglo American suggest that briquetting could increase process safety and stability by reducing gas build-up, boost nameplate capacity by 3 kt/a, and lower plant electricity consumption by 5% [12].

During the briquetting process, fines are pressed into lumps of regular shapes using either rolls, extruders, or punches [6]. Briquetting utilises three main techniques, vibro-pressing, extrusion, and roller pressing, each differing in forming pressure, briquette shape, strength, and machine capacity. Vibro-pressing briquetting technology, which combines mechanical vibration and high-pressure compaction, was first introduced in 1970. In its first application, this technology was used for the agglomeration of agricultural raw material [10]. Vibro-pressing produces briquettes at relatively low pressures, in the range of 0.02–0.1 MPa, and a frequency of 30–70 Hz. Typical vibro-pressing briquetting equipment has a maximum capacity of 30 t/h [10]. This technology produces rectangular or pillow-shaped briquettes with relatively low mechanical strength, which are not suitable for transport via conveyor belts. Extrusion as a method of agglomerating iron ore fines was first practiced in the 1950s. In its first application, a hydrated mixture of iron ore fines and bentonite was placed in a chamber and then extruded through a die, producing cylindrical briquettes [10]. Extrusion briquetting is primarily used to produce dense, spherical agglomerates with good integrity. The largest particle size suitable for this technology is 5 mm [10]. The key criterion for determining whether a material is suitable for extrusion is its plasticity, as this property ensures that the material can be successfully forced through the die openings. Roller-press technology was originally developed for briquetting fine iron ore particles and metallurgical waste. It is typically limited to producing pillow- or egg-shaped agglomerates, as spherical briquettes require hemispherical pockets that promote sticking, making them unsuitable for this design. A roller-press briquetting machine consists of two counter-rotating rollers within a steel frame. Material is fed into the roller gap either by gravity or screw feeding. Uniform and continuous feeding is essential to ensure consistent filling of the nip region and the formation of homogenous briquettes [13].

Johanson's theory identifies three distinct regions in roller compaction: slip, nip, and release [14]. Compaction occurs in the nip region, where the roller gap is narrowest. Initially, particles enter the slip region, characterised by movement along the roller surface, influenced by wall and inter-particle friction [13]. The nip region begins at the roll angle, α, where particle velocity equals roller speed, drawing material into the compression zone. Increasing the nip angle raises the pressure applied while reducing the roller speed and

gap. In the release region, as the gap widens, briquettes exit the press and may expand slightly due to elastic recovery, resulting in the strip thickness exceeding the roller gap. A comparison of different briquetting technologies is shown in Table 1.

Table 1. Comparison of briquetting technologies [10,13,14].

Parameter	Briquetting Type		
	Vibro-Press	Extruder	Roller-Press
Feed mechanism	Manual or vibratory filling	Ram-feed or gravity-feed extruders	Gravity or screw feeding into rolls
Product strength	Low mechanical strength	High mechanical integrity and density	Moderate to high strength, depending on roll pressure
Material size suitability	Fine and natural materials	Coarse	Fine powders and particles
Production rate	Up to 30 tons/hour	Variable, dependent on extruder and feed type	High capacity is possible, depending on roll size and speed
Process type	Semi-continuous or batch	Continuous (four-step process)	Continuous (can also operate in batch or semi-batch)

2.2. Binders in Briquetting

Binders are typically used in the production of briquettes. These binders should provide strong bonding and be pollution-free, environmentally friendly, and cost-effective [15]. Organic binders, inorganic binders, and composite binders are used. Common inorganic binders include clay, lime, plaster, cement, and sodium silicate, while organic binders include biomass, tar pitch, petroleum bitumen, lignosulphonate, and polymers [16]. Composite binders combine two or more types of binders, typically organic and inorganic binders, to exploit their respective advantages.

Binderless briquetting has emerged as a replacement technology for cold-press briquetting with a binder [17,18]. This process relies on the natural bonding of particles under high pressure. Binderless briquetting is associated with easier logistics, reduced production costs, simplified process routes, and higher-purity briquettes with associated environmental benefits, making it an efficient and sustainable choice.

2.3. Briquette Performance

The quality of briquettes and effectiveness of briquetting can be influenced by various factors. These factors fall into two main categories: machine properties and ore properties.

Machine properties refer to characteristics of the briquetting machine itself, such as the speed of the rolls of the machine and the pressure applied by the rolls. Ore properties refer to characteristics of the material being briquetted; these include the particle size distribution (PSD), the moisture present in the material, and the conditions under which the material is cured [11,19].

2.4. Roll Pressure

A study on compacting oak sawdust found that increasing pressure led to higher resistance to abrasion and impact, as well as greater compressive strength, in the resulting agglomerates [20]. Vining et al. (2017) studied the impact of machine roll speed on the production of green briquettes using Australian hematite–goethite iron ore fines with varying moisture contents [11]. The findings showed that briquettes made at a roll speed of 12 rpm were weak and poorly formed and had low yield. It was concluded that roll speeds between 4.5 and 10 rpm were optimal for producing satisfactory quality briquettes.

2.5. Particle Size Distribution

Finer particles create more contact points between them, resulting in stronger bonds and higher compressive strength. This is because smaller particles reduce the distance between each other, increasing the forces between them [19]. Kaliyan and Morey (2009) observed that reducing the average size of rice husks from 5.14 mm to 4.05 mm improved briquette durability from 84.1% to 95% when compressed at 31.2 MPa [20].

2.6. Moisture Content

Various studies have shown that the strength of ores is compromised in the presence of water. Several explanations have been suggested for this effect, including fracture energy reduction and pore water pressure [21]. As moisture content increases, the fluids within the pores of a particle can become pressurised during compression, creating an outward pressure gradient [21]. This pressure gradient weakens the strength of the ore. The pore pressure is influenced by the effective stress, which plays a role in the strength of ore containing interconnected pores.

3. Materials and Methods

3.1. Materials

Samples of ferronickel ore were received from Barro Alto, packaged in 200 L drums. The ore was dried at 105 °C to a constant mass. After drying, the samples were homogenised and rotary-split into three fractions: the ROM ore and –6.3 mm and –12.5 mm samples. These three fractions were each reserved for chemical and mineralogical characterisation. Operational parameters (particle size distribution and moisture) were selected to align with those used at Anglo American's Barro Alto plant. Moisture contents of 16% and 24% are typical for operating nickel laterite plants; Loma de Niquel, Venezuela, operates at a moisture content of 15%, whilst Pacific Metal Co., Chiyoda, Japan, operates at a moisture content of 24% [22].

The inherent moisture content was determined for each 20 kg batch using an MB-90-OHAUS moisture content analyser. These values were then used to calculate the required water additions to achieve moisture contents of 16% and 24%.

3.2. Briquette Production

Pillow-shaped binderless briquettes were produced with dimensions of 30 mm × 30 mm × 18 mm (W × L × H), using ore with a top size of −6.3 mm. For the ore with a top size of −12.5 mm, the dimensions of the briquettes were 30 mm × 30 mm × 20 mm. Both sets of briquettes were allowed to cure for a period of 2 h prior to the ISO tests, in line with Anglo American's standards. The closed-cured briquettes were placed in a sealed chamber; the open-cured briquettes were placed on a tray and cured in the open atmosphere.

3.3. Briquette Characterisation

Several standard tests have been developed by the International Standards Organisation (ISO) to evaluate the quality of iron ore lump, pellets, and sinter; however, no standard tests exist for evaluating the performance of ferronickel briquettes [23]. For the current study, the determination of the performance of the briquettes was determined using the ISO standard procedures for iron ore pellets, as shown in Table 2. In these ISO test methods, two determinations (repeats) are typically performed per sample to evaluate the repeatability and ensure the reliability of the test results.

Table 2. ISO standards for briquette characterisation.

Standard	Test ID		Target
ISO 4700 [24]	Compressive strength	CS(N)	350–620
ISO 3271 [25]	Tumble strength Abrasion index	TI (% > 6.3 mm) AI (% −0.5 mm)	95.5–96.2 2.93–3.57
ISO 4695 [26]	Reducibility index	RI (%)	39.3–42.2
ISO 8371 [27]	Decrepitation index	DI (% −3.15 mm)	0.083–0.22
ISO 4696-1 [28]	Reduction disintegration index	RDI (% −3.15 mm)	1.60–8.95
Non-standard test	Linder furnace (laboratory rotary furnace) degradation	Mass% −3.15 mm	2.67–5.60

3.4. Design of Experiments

The current study adopted a Design of Experiments (DoE) approach to systematically evaluate the effects of key variables on the briquette performance. A DoE allows valid conclusions to be drawn even in the presence of natural fluctuations such as temperature, soil conditions, and rainfall [29]. A two-level factorial design was used, enabling all factors to vary in each experiment and allowing both individual and interaction effects to be assessed [30].

In this study, three factors were tested at two levels—moisture content, top size, and curing conditions—resulting in $2^3 = 8$ briquette production tests. This factorial design ensured efficient analysis of the factor effects and their interactions. The evaluation was conducted using a statistical software package (Minitab 19.1), and main effects plots were used in the analysis. The test matrix is shown in Table 3.

Table 3. Briquette production test matrix.

Test Number	Moisture, %	Ore Top Size, mm	Curing Condition
1	16	−6.3	Open
2	24	−6.3	Open
3	16	−12.5	Open
4	24	−12.5	Open
5	16	−6.3	Closed
6	24	−6.3	Closed
7	16	−12.5	Closed
8	24	−12.5	Closed

4. Results

Characterisation of Ore Samples

The characterisation of the ore samples included particle size distribution analysis, assay-by-size analysis, bulk elemental analysis, and mineralogical analysis (using powder X-ray diffraction (XRD) and scanning electron microscopy (SEM) employing energy dispersive spectrometry (EDS)).

X-ray fluorescence (XRF) analysis was carried out using a Malvern Panalytical Axios FAST (Malvern Panalytical) to determine the chemical compositions. The Malvern Panalytical Axios FAST is a wavelength-dispersive X-ray fluorescence (WDXRF) spectrometer intended for rapid elemental analysis in solid and fused materials. The crystalline phase compositions of the ore were determined by X-ray diffraction (XRD) analysis using a PANalytical X'Pert Pro powder diffractometer in the θ–θ configuration with an X'Celerator

detector and variable divergence and fixed receiving slits with Fe-filtered Co-Kα radiation (λ = 1.78 × 10^{-6} mm). The relative phase amounts (mass% of crystalline phase) were estimated using the Rietveld method (Autoquan 5.0 software, Meyer Instruments, United States of America).

The XRF analysis of the feed (ROM) sample (Table 4) showed that the ore contained 2.03 mass% of NiO and 17.2 mass% of Fe_2O_3. Considering its average $(SiO_2)/(Al_2O_3 + Fe_2O_3)$ mass ratio of 2.08, the ore was classified as lateritic. According to Janwong (2012), lateritic ores typically consist of 0.4–3 mass% Ni, 0.02–1 mass% Co, 10–30 mass% Mg, and 9–25 mass% Fe [31]. The XRF analysis confirmed that the ROM ore was a saprolitic laterite, with 12.0 mass% Fe, 17.2 mass% Mg, and 1.60 mass% Ni. Lu et al. (2013) noted that hydrous magnesia silicates dominate saprolites, with nickel substituting magnesium to form garnierite $(Mg,Ni)_3Si_2O_5(OH)_4$ without any discrete nickel minerals [32].

Table 4. X-ray fluorescence analysis of the ROM sample and different size fractions (−6.3 mm and −12.5 mm).

	Component, Mass %		
Analyte	**ROM**	**−6.3 mm Fraction**	**−12.5 mm Fraction**
SiO_2	41.6	37.6	44.2
Al_2O_3	2.8	4.18	2.67
Fe_2O_3	17.2	21.9	14.2
NiO	2.03	2.15	1.93
MgO	23	19.4	28.8
Fe (Total)	12	15.3	9.93
Ni (total)	1.6	1.69	1.52
Fe/Ni	7.54	9.07	6.55
$(SiO_2)/(Al_2O_3 + Fe_2O_3)$	2.08	1.44	2.62
LOI	11	12.4	11.1

The ROM sample consisted of a 7.80 mass% of particles below 600 µm and a 0.40 mass% below 25 µm. For the ore with a top size of −6.3 mm, the XRF analysis revealed 2.15 mass% NiO and a loss on ignition (LOI) of 12.4%. Screening therefore increased the NiO content to 5.9% and the Fe_2O_3 to 27.3%, indicating rejection of the nickel-lean minerals. However, for the ore with a top size of −12.5 mm, the analysis showed 1.93 mass% NiO with an LOI of 11.1%.

This represents a decrease of 4.9 mass% in the NiO content and 17.4 mass% in the Fe_2O_3 content compared to the plant feed. With a $(SiO_2)/(Al_2O_3 + Fe_2O_3)$ mass ratio of 2.62, the −12.5 mm fraction was categorized as a non-lateritic, tropically weathered ore rather than a true laterite. According to Crundwell et al. (2011), screening offers a cost-effective method to reject nickel-lean minerals compared to leaching [22].

The quantitative XRD analyses of the ROM, −6.3 mm, and −12.5 mm feed samples are shown in Table 5. The results indicate that the ore primarily consists of silicates: lizardite $(Mg_3Si_2O_5(OH)_4)$ from the serpentine group, quartz (SiO_2) as a framework silicate, and forsterite $(Mg_{1.8}Fe_{0.2}SiO_4)$ from the olivine group. Iron is predominantly found in non-silicate minerals, specifically hematite (Fe_2O_3) and magnetite (Fe_3O_4). In the case of the −6.3 mm ore top size, the results show a notable 18.1% decrease in the mass% of quartz (from 11.8% to 9.66%). Additionally, magnesium-rich olivine (forsterite), which poses challenges during smelting, is also reduced by 18.7% (from 6.36% to 5.17%). Gleeson et al. (2004) confirmed that saprolites are dominated by an amorphous phase [33]. Work by Bolaños-Benítez et al. (2020), who studied the potential release of chromium from solids to surface water and groundwater in a nickel laterite deposit from Barro Alto, also noted the presence of an amorphous phase [3].

Table 5. Quantitative X-ray diffraction analysis of the ROM sample and different size fractions (−6.3 mm and −12.5 mm).

	Mineral, Mass %		
Mineral	**ROM**	**−6.3 mm Fraction**	**−12.5 mm Fraction**
Amorphous	34.3	40.7	15.2
Chlorite	6.51	6.53	15
Enstatite	1.37	4.14	5.7
Forsterite	6.36	5.17	16.2
Hematite	1.30	2.96	1.30
Hornblende	5.40	6.88	3.10
Lizardite	22.8	18.8	18.0
Magnetite	4.19	5.16	-
Quartz	11.8	9.66	11.3
Talc	5.9	–	14.2

5. Characterisation of Briquettes

5.1. Compressive Strength

When comparing the compressive strength of the briquettes across the different size fractions, the results indicated that higher compressive strength was observed with lower moisture content (Figure 2). This relationship is attributed to the Rhebinder effect, where an increase in moisture content leads to a decrease in surface energy due to physical absorption, resulting in reduced strength. Additionally, the results revealed that the compressive strength increased with the decreasing ore top size of the briquettes. This is because finer particles experience greater inter-particle forces, which in turn enhance the strength of the briquettes [34]. Only the −6.3 mm briquettes with 16% moisture, cured under open conditions, exceeded the minimum targeted compressive strength of 350 N for iron ore pellets (Table 2).

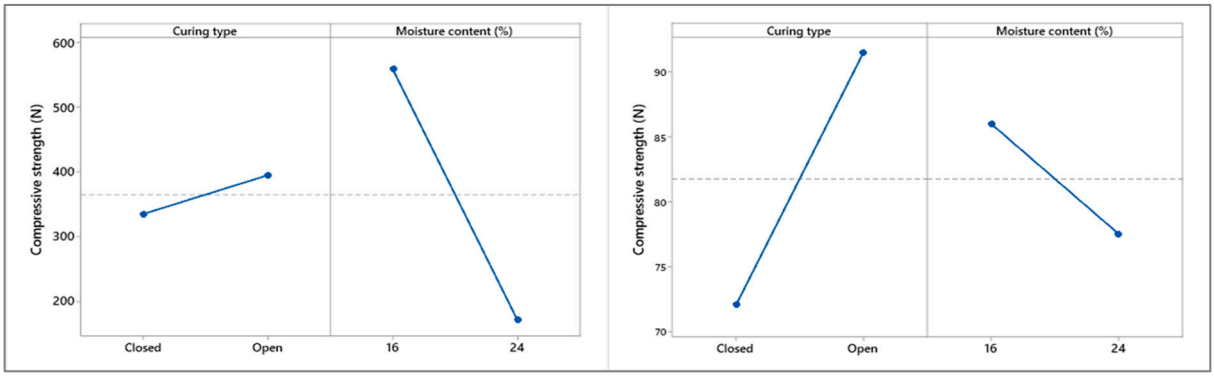

Figure 2. Main effects plot for green briquette compressive strength: −6.3 mm, (**left**); −12.5 mm, (**right**).

5.2. Tumble Index and Abrasion Index

The tumble strength (TI) and abrasion index (AI) test results showed that both indices decreased as the moisture content increased. These findings are consistent with the findings of Xue et al. (2022), who studied the effect of moisture content on limonitic nickel laterites and found that increasing the moisture content from 14% to 21% had a beneficial effect on the TI, but at moisture contents greater than 21%, the TI deteriorated [35]. The main effects plot, shown in Figure 3, indicates that at a briquette ore top size of −6.3 mm, the moisture content has a greater significance on the TI than the curing condition. At a briquette ore top size of −12.5 mm, the curing conditions have a more significant impact on the TI. The main-effects plots for the abrasion index (Figure 4) indicate that for both briquette ore top sizes,

the curing conditions have far greater significance on the AI than the moisture content. The results indicate that the lowest AI was obtained under open curing conditions. The highest TI (% > 6.3 mm) and the lowest AI (% < 0.5 mm) were observed for the −6.5 mm briquettes with 16% moisture, cured under open conditions. However, the TI was lower than the minimum targeted TI (% > 6.3 mm) of 95.5 for iron ore pellets, while the AI exceeded the maximum AI (% < 0.5 mm) of 3.57 for iron ore pellets (Table 2).

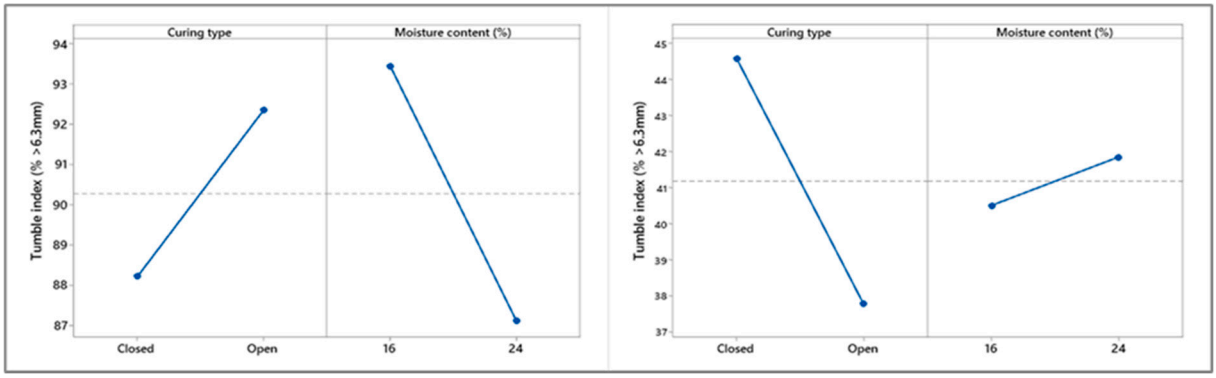

Figure 3. Main effects plot for tumble strength: −6.3 mm, (**left**); −12.5 mm, (**right**).

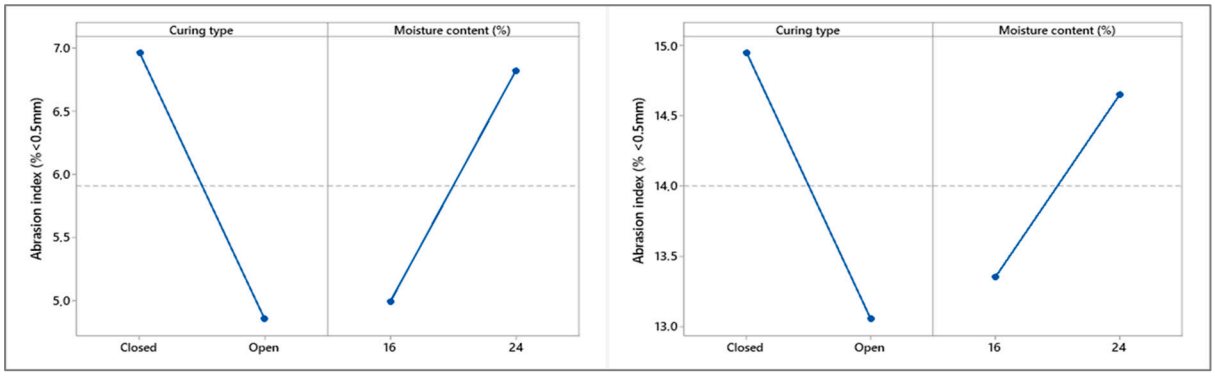

Figure 4. Main effects plot for abrasion index: −6.3 mm, (**left**); −12.5 mm, (**right**).

5.3. Reducibility Index

The reducibility index test results, shown in Table 6, indicate a decrease in the degree of reduction with an increase in the moisture content. These results indicate a similar trend to that observed by Goenka and Naik (2013), who noted a decrease in the degree of iron reduction with an increase in moisture content from 13% to 15% [36].

Table 6. Reducibility index test results.

Briquette Ore Top Size	Moisture, %	Curing Condition	Average Mass Loss, g	Average Reduction, %
−6.3 mm	16	Open	132.5	33.4
	16	Closed		
	24	Open	165.1	27.6
	24	Closed		
−12.5 mm	16	Open	124	39.9
	16	Closed		
	24	Open	135	37.5
	24	Closed		

Murakami et al. (2009) and Li (1999) also asserted that an increase in moisture content had a detrimental effect on the degree of reduction, with the latter attributing this effect to the presence of water vapour [5,37]. Only the −12.5 mm briquettes with 16% moisture content had a reducibility index within the targeted range of 39.3%–42.2% for iron ore pellets (Table 2).

5.4. Decrepitation Index

The likelihood of briquette disintegration and fines formation increased with an increase in moisture content. At 16% moisture, an average mass disintegration (mass% of −0.5 mm particles) of 0.09% was reported; this value increased to 0.16% at 24% moisture, indicating a 43.8% increase in fines generation.

In a study on the behaviour of briquettes manufactured from the Azul and Urucum deposits in Brazil, Faria et al. (2010) concluded that ores with higher moisture contents exhibited greater decrepitation intensity than those with lower moisture contents [38]. At a briquette ore top size of −12.5 mm, the results indicated a marginal decrease in the DI with increasing moisture content: an average DI of 2.34% was reported for the 16% moisture, which decreased to 1.96% for the 24% moisture.

The likelihood of briquette disintegration, resulting in the formation of fines, decreased slightly with increasing moisture content. The average mass disintegration values (mass% −0.5 mm) of 0.36% and 0.26% were measured at 16% and 24% moisture content, respectively, indicating a 28.6% decrease in fines generation.

The main-effects plots indicate that for a briquette ore top size of −6.3 mm, the moisture content had a greater significance on the DI than the curing conditions; the opposite was true for the briquette ore top size of −12.5 mm (Figure 5).

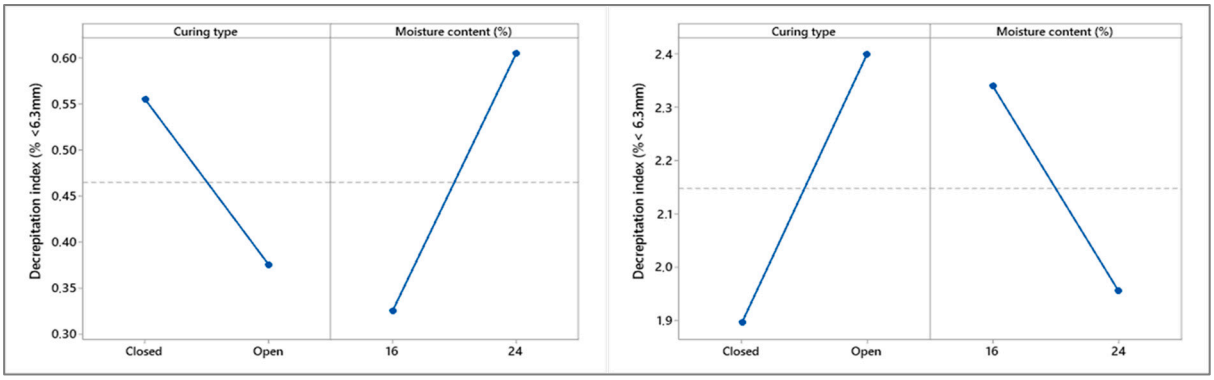

Figure 5. Main effects plot for decrepitation index: −6.3 mm, (**left**); −12.5 mm, (**right**).

5.5. Reduction Disintegration Index

The reduction disintegration results (Table 7) show that with an increase in the briquette ore top size, the briquette disintegration increases. Larger particles are more susceptible to defects and cracks, acting as stress points that enhance briquette deterioration during reduction. The disintegration of the briquettes in the low-temperature reduction zone of the furnace shaft is primarily attributed to crack initiation and propagation because of the volume change associated with the reduction of hematite to magnetite [39]. The quantitative X-ray diffraction analysis of the briquettes after the reduction disintegration index tests, shown in Table 8, confirmed the reduction of hematite to magnetite. The −6.3 mm briquettes with both 16% and 24% moisture content had reduction disintegration indexes ($RDI_{-3.15\ mm}$) within the targeted range of 1.60%–8.95% for iron ore pellets (Table 2).

Table 7. Reduction disintegration test results.

Briquette Ore Top Size −6.3 mm					
Moisture, %	**Curing Condition**	**Reduction Disintegration Index,**			
		$RDI_{+6.3\ mm}$	**$RDI_{-3.15\ mm}$**	**$RDI_{-0.5\ mm}$**	
16	Open	97.6	2.24	1.59	
16	Closed	96.9	2.93	1.93	
Average		**97.3**	**2.59**	**1.76**	
24	Open	96.9	3.03	2.54	
24	Closed	92.4	6.54	4.11	
Average		**94.7**	**4.79**	**3.33**	
Briquette Ore Top Size −12.5 mm					
Moisture, %	**Curing Condition**	**Reduction Disintegration Index,**			
		$RDI_{+6.3\ mm}$	**$RDI_{-3.15\ mm}$**	**$RDI_{-0.5\ mm}$**	
16	Open	79.8	14.4	7.00	
16	Closed	78.3	14.3	6.53	
Average		**79.1**	**14.4**	**6.77**	
24	Open	69.4	16.9	6.35	
24	Closed	72.7	17.7	7.8	
Average		**71.1**	**17.3**	**7.08**	

Table 8. Average quantitative X-ray diffraction analysis of briquettes after reduction disintegration tests.

Phase ID	**Mineral Mass, %**			
	Briquette Ore Top Size −6.3 mm		**Briquette Ore Top Size −12.5 mm**	
	Moisture Content		**Moisture Content**	
	16%	**24%**	**16%**	**24%**
Amorphous	31.1	40.4	26.6	21.2
Clinochlore	7.03	5.58	14.6	15.5
Diopside	1.55	1.53	-	-
Enstatite	9.33	8.22	5.45	6.35
Forsterite	5.61	4.59	-	-
Hornblende	5.52	3.62	2.45	2.80
Lizardite	16.9	15.7	21.7	23.4
Magnetite	8.68	8.60	5.05	5.05
Quartz	8.47	6.89	8.05	7.80
Talc	5.85	4.92	15.9	18.0

5.6. Linder Reactor

Linder reactor tests were performed to simulate the conditions within a rotary kiln, aiming to assess the degradation of green briquettes during tumbling, heating, calcination, and reduction. The results (Table 9) show that the disintegration of the briquettes, resulting in the generation of fines (mass% −0.5 mm), increases with the briquette ore top size. These findings are similar to those observed by Rojas Arias et al. (2018), who reported that disintegration increased with an increase in particle size when a sample was subjected to Linder reactor conditions [40]. An increase in briquette disintegration was observed with the increasing moisture content. These findings indicate that while moisture can act as a binder, excessive moisture may weaken the bonds between particles, leading to higher disintegration. It can be inferred that higher moisture concentrations may cause greater swelling, which increases porosity, making the briquettes more susceptible to disintegration and generating excessive fines.

Table 9. Linder reactor briquette disintegration.

Briquette Ore Top Size	Moisture, %	Curing Condition	Average Mass Disintegration Index, % +6.3 mm	−3.15 mm	−0.5 mm
−6.3 mm	16	Open	95.3	4.50	3.80
	16	Closed			
	24	Open	70.3	21.4	11.3
	24	Closed			
−12.5 mm	16	Open	25.4	50.3	25.1
	16	Closed			
	24	Open	30.3	45.5	19.8
	24	Closed			

The main effects and interaction plots for the briquette mass disintegration are shown in Figures 6 and 7 and in Figures 8 and 9, respectively. The main effects plot shows that the moisture content was the most influential factor for both briquette ore top sizes, while the curing conditions had a minimal impact on the briquette disintegration. For the briquette ore top size of −6.3 mm, the interaction plots show no interaction between the moisture content and curing conditions in terms of briquette disintegration (both mass% +6.3 mm and mass% −0.5 mm). However, for the −12.5 mm ore top size, there is a strong interaction between these variables for both size fractions. For the −12.5 mm top size, the optimal briquette disintegration conditions occur with 24% moisture content and open curing conditions. Only the −6.3 mm briquettes with 16% moisture content had a Linder disintegration index within the targeted range of 2.67%–5.60% for iron ore pellets (Table 2).

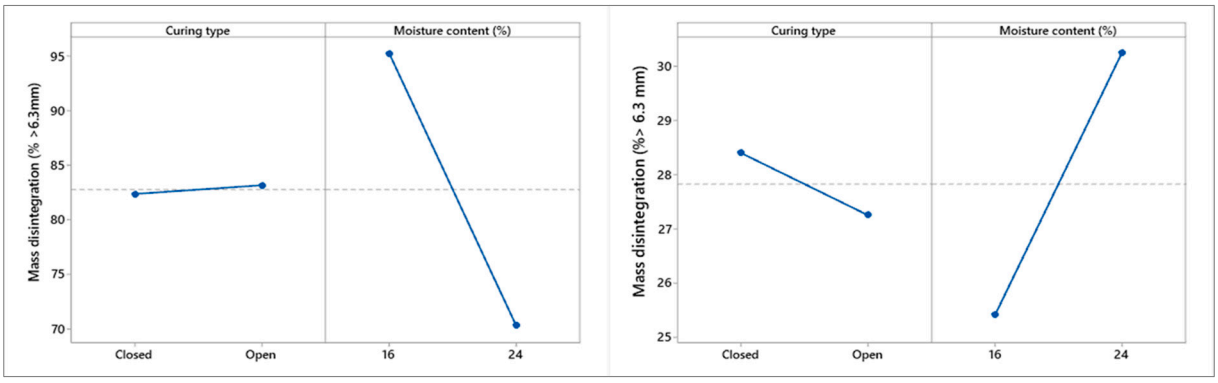

Figure 6. Main effects plot of mass disintegration (+6.3 mm): −6.3 mm, (**left**); −12.5 mm, (**right**).

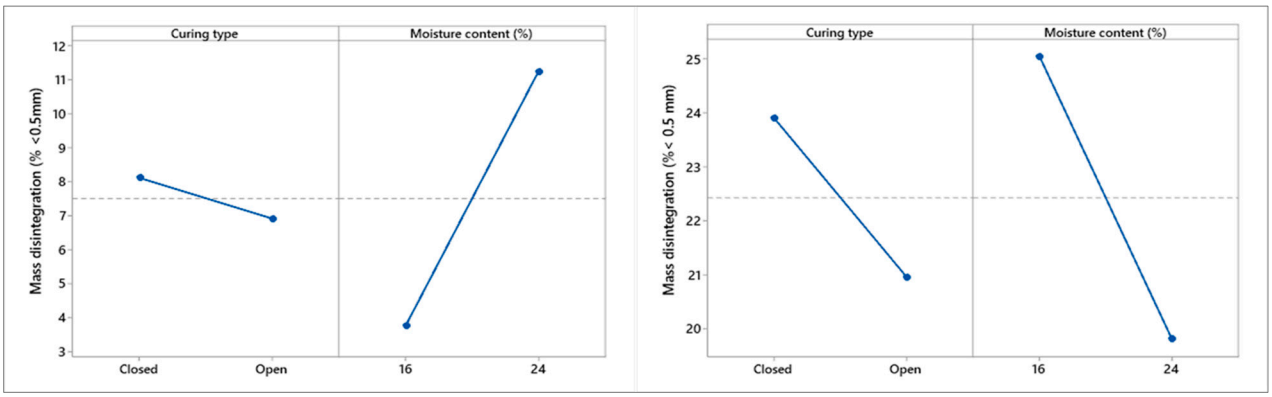

Figure 7. Main effects plot of mass disintegration (−0.5 mm): −6.3 mm, (**left**); −12.5 mm, (**right**).

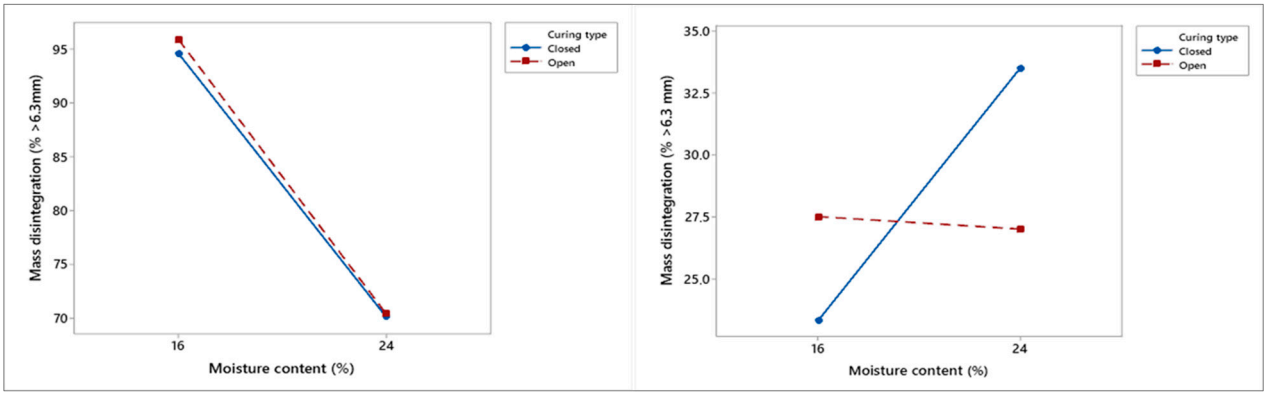

Figure 8. Interaction plot of mass disintegration (+6.3 mm): −6.3 mm, (**left**); −12.5 mm, (**right**).

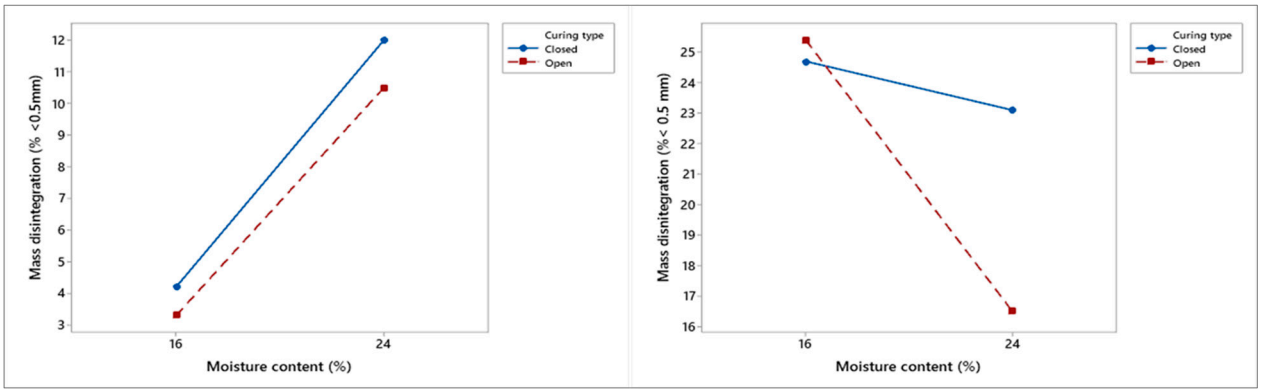

Figure 9. Interaction plot of mass disintegration (−0.5 mm): −6.3 mm, (**left**); −12.5 mm, (**right**).

6. Discussion

The X-ray fluorescence (XRF) analysis of the ore identified it as saprolitic laterite. Lu et al. (2013) stated that hydrous magnesia silicates dominate saprolites, with nickel substituting magnesium to form garnierite $(Mg,Ni)_3Si_2O_5(OH)_4$ without any discrete nickel minerals [32]. Upgrading the nickel content in laterites is typically achieved through the selective removal of silica or rejection of low-grade constituents, a process often accompanied by changes in ore chemistry [41]. A comparison of XRF analysis between the ROM, −6.3 mm, and −12.5 mm fractions indicated better ore upgrading when screened at −6.3 mm.

The ROM sample contained 2.03 mass% NiO and 17.2 mass% Fe_2O_3, while screening at −6.3 mm resulted in improved grades of 2.15 mass% NiO and 21.9 mass% Fe_2O_3, compared with the 1.93 mass% NiO and 14.2 mass% Fe_2O_3 in the −12.5 mm fraction.

This study highlights the significance of ore top size and particle size distribution on the briquetting process and the performance of briquettes. Fine particles are essential to the binding mechanism during briquette formation; however, their presence reduces permeability, negatively impacting furnace performance. This reduction in permeability leads to lower metal extraction rates and increased power consumption [36]. Additionally, fine particles increase the potential for gas build-up, compromising both process safety and stability [42]. The tumble index (TI) test results indicated that the TI decreases with increases in both moisture content and briquette ore top size.

For a briquette ore top size of −6.3 mm, average TI values of 93.5% and 87.6% were reported for the moisture contents of 16% and 24%, respectively. For the −12.5 mm ore top size, the respective values were 40.5% and 41.9%. This trend demonstrates that larger ore top sizes and higher moisture contents negatively impact the structural integrity of briquettes.

Additionally, the green briquette compressive strength was significantly affected by both the moisture content and ore top size. For the −6.3 mm briquettes, average strengths of 480 N and 155 N were recorded at 16% and 24% moisture, respectively, while the −12.5 mm briquettes showed much lower values of 125 N and 75.9 N. This confirms that finer particles promote better green strength, which is crucial for handling and processing. The lower TI values imply that the briquettes were less resistant to mechanical degradation during handling and transportation. This could negatively affect machine performance, leading to blockages, irregular material flow, and increased maintenance requirements. Similarly, the abrasion index (AI) tests showed an increase in the AI with the briquette ore top size, which adversely affects the permeability. For the −6.3 mm briquettes, an AI of 5.91% was reported, while the −12.5 mm briquettes exhibited a much higher AI of 14.0%, representing a 136.8% increase.

The reducibility test results showed that the briquettes produced at the ore top size of −12.5 mm had slightly higher porosity, leading to improved gas and temperature permeability. Density analysis confirmed a marginally lower density for the −12.5 mm briquettes (2.357 g/cm^3), supporting the observation that those briquettes had higher porosity, contributing to better reducibility. For the −6.3 mm briquettes, average degrees of reduction of 33.4% and 27.6% were reported for the 16% and 24% moisture content, respectively, while the −12.5 mm briquettes showed slightly higher reduction values of 39.2% and 36.9%. This increase in the reducibility with the ore top size may be linked to improved porosity and enhanced gas flow through the briquettes. However, the presence of finer particles in the −6.3 mm feed likely hindered the gas permeability, reducing the overall reduction efficiency despite better green strength. Increasing the briquette ore top size from −6.3 mm to −12.5 mm had adverse effects on the reduction disintegration index (RDI), with the RDI+6.3 mm values dropping by 21.8%. The RDI measurements further confirmed the impact of the ore top size on the thermal stability, with −6.3 mm briquettes yielding an average RDI+6.3 mm of 96.0% compared with 75.1% for the −12.5 mm briquettes. Additionally, the RDI−0.5 mm increased from 2.54% to 6.92%, indicating greater disintegration for coarser briquettes.

Furthermore, the average mass disintegration (mass% −0.5 mm) in the Linder furnace test increased from 7.50% for the −6.3 mm briquettes to 22.4% for the −12.5 mm briquettes, indicating that the larger briquettes were more prone to disintegration and the formation of fine particles during reduction. These results suggest a trade-off between strength and reducibility: while larger briquettes (−12.5 mm) exhibit better gas permeability and reduction performance due to increased porosity, they suffer from lower mechanical stability and greater disintegration under thermal load.

7. Conclusions

The purpose of this study was to evaluate the performance of binderless briquettes as a potential feed for the electric arc furnaces at the Barro Alto operation. This study considered three key parameters in evaluating the performance of the briquettes: the particle size distribution of the feed to the briquetting process (−6.3 mm and −12.5 mm), moisture content (16% and 24%), and curing conditions (open and closed). The following conclusions can be drawn:

Screening of the ROM ferronickel ore rejected nickel-lean minerals. Ore with a top size of −6.3 mm had an improved grade of 2.2 mass % NiO compared with the 2.0 mass % NiO in the ROM ore.

Binderless briquettes with sufficient physical properties can be produced from Barro Alto ferronickel ore.

Moisture content is the most influential factor on the properties of briquettes, while curing conditions have a minimal impact.

For optimal process safety and stability, briquettes should be produced with an ore top size of −6.3 mm and a moisture content of 16% and cured under open curing conditions, as these parameters yield the briquettes with the highest structural integrity.

Although briquettes with ore top sizes of −12.5 mm and moisture content of 16% had the highest reducibility, these briquettes had excessively high reduction disintegration indexes ($RDI_{-3.15\,mm}$), which make them unfavourable for use.

Author Contributions: Conceptualisation, N.N.; methodology, J.O.M., N.N. and A.M.G.-C.; experimental work: J.O.M.; validation, J.O.M., N.N. and A.M.G.-C.; writing—original draft preparation, J.O.M.; writing—review and editing, N.N. and A.M.G.-C.; supervision, N.N. and A.M.G.-C.; project administration, A.M.G.-C.; funding acquisition, A.M.G.-C. All authors have read and agreed to the published version of the manuscript.

Funding: This project was funded by Anglo American Value-In-Use, Technical Solutions, Johannesburg, South Africa.

Data Availability Statement: Data supporting the reported results can be provided upon request.

Acknowledgments: The authors would like to thank Anglo American Value-In-Use for their financial support. Special thanks are also due for Jacques Muller from Anglo American Value-In-Use for his technical insights, as well as the assistance from the staff of the Department of Materials Science and Metallurgical Engineering, University of Pretoria.

Conflicts of Interest: The authors have no conflicts of interest to declare.

References

1. Anglo American. Anglo American Analyst Visit 2009. 2009. Available online: https://www.angloamerican.com/~/media/Files/A/Anglo-American-Group/PLC/media/presentations/2009pres/barro_alto_visit/barro_alto_visit.pdf (accessed on 12 November 2024).
2. Ratié, G.; Garnier, J.; Calmels, D.; Vantelon, D.; Guimarães, E.; Monvoisin, G.; Nouet, J.; Ponzevera, E.; Quantin, C. Nickel distribution and isotopic fractionation in a Brazilian lateritic regolith: Coupling Ni isotopes and Ni K-edge XANES. *Geochim. Cosmochim. Acta* **2018**, *230*, 137–154. [CrossRef]
3. Bolaños-Benítez, V.; Van Hullebusch, E.D.; Birck, J.-L.; Garnier, J.; Lens, P.N.L.; Tharaud, M.; Quantin, C.; Sivry, Y. Chromium mobility in ultramafic areas affected by mining activities in Barro Alto massif, Brazil: An isotopic study. *Chem. Geol.* **2021**, *561*, 120000. [CrossRef]
4. International Nickel Study Group. *World Nickel Factbook 2021*; INSG: Lisbon, Portugal, 2022. Available online: https://insg.org/wp-content/uploads/2022/02/publist_The-World-Nickel-Factbook-2021.pdf (accessed on 12 November 2024).
5. Li, S. Study of Nickeliferrous Laterite Reduction. Master's Dissertation, Faculty of Engineering, McMaster University, Hamilton, ON, Canada, 1999.
6. Eisele, T.C.; Kawatra, S.K. A review of binders in iron ore pelletization. *Miner. Process. Extr. Metall. Rev.* **2003**, *24*, 1–90. [CrossRef]
7. Brosig, D.; Safe, P.; Russell, M.; Arévalo, J.; Kiyan, C.; Rodrigues, M.; Miranda, M. Decarbonization at the Anglo-American Barro Alto smelter through implementation of the Ecombustible technology. In Proceedings of the 61st Conference of Metallurgists, COM 2022, Montréal, Quebec, Canada, 21–24 August 2022; Springer: Cham, Switzerland, 2023; pp. 939–948. [CrossRef]
8. Vale. Vale begins Load Tests in the First Iron Ore Briquette Plant in Brazil. Vale Now Press. 31 August 2023. Available online: https://www.vale.com/w/vale-begins-load-tests-in-the-first-iron-ore-briquette-plant-in-brazil (accessed on 7 November 2023).
9. Anglo American. Climate Change Report. 2022. Available online: https://www.angloamerican.com/~/media/Files/A/Anglo-American-Group-v5/PLC/investors/annual-reporting/2022/climate-change-report-2022.pdf (accessed on 12 November 2024).
10. Kurunov, I.; Bizhanov, A. Features of Stiff Vacuum Extrusion as a Method of Briquetting Natural and Anthropogenic Raw Materials. In *Stiff Extrusion Briquetting in Metallurgy*; Topics in mining, metallurgy and materials engineering; Springer: Berlin/Heidelberg, Germany, 2018; pp. 23–68. [CrossRef]
11. Vining, K.R.; Khosa, J.; Sparrow, G.J. Briquetting conditions for Australian hematite-goethite iron ore fines. *ISIJ Int.* **2017**, *57*, 1517–1523. [CrossRef]

12. Brujin, W. Brazil: Minas-Rio and Nickel: Bulks Seminar and Site Visit. Brisbane. 2019. Available online: https://www.angloamerican.com/~/media/Files/A/Anglo-American-Group/PLC/media/presentations/2019pres/minas-rio-and-nickel.pdf (accessed on 12 November 2024).
13. Kleinebudde, P.; Knop, K. Direct pelletization of pharmaceutical pellets in fluid-bed processes. In *Handbook of Powder Technology, Volume 11: Granulation*; Elsevier: Amsterdam, The Netherlands, 2007; Volume 11, Chapter 17; pp. 799–811. [CrossRef]
14. Souihi, N. Multivariate Synergies in Pharmaceutical Roll Compaction: The Quality Influence of Raw Materials and Process Parameters by Design of Experiments. Doctoral Thesis, Department of Chemistry, Umeå University, Umeå, Sweden, 2014.
15. Zhang, G.; Sun, Y.; Xu, Y. Review of briquette binders and briquetting mechanism. *Renew. Sustain. Energy Rev.* **2018**, *82*, 477–487. [CrossRef]
16. Obi, O.F.; Pecenka, R.; Clifford, M.J. A review of biomass briquette binders and quality parameters. *Energies* **2022**, *15*, 2426. [CrossRef]
17. Han, Y.; Taymasebi, A.; Yu, J.; Li, X.; Meesri, C. An experimental study on binderless briquetting of low-rank coals. *Chem. Eng. Technol.* **2013**, *36*, 749–756. [CrossRef]
18. Olugbade, T.O.; Ojo, O.T. Binderless briquetting technology for lignite briquettes: A review. *Energy Ecol. Environ.* **2021**, *6*, 69–79. [CrossRef]
19. Sun, B.; Yu, J.; Tahmasebi, A.; Han, Y. An experimental study on binderless briquetting of Chinese lignite: Effects of briquetting conditions. *Fuel Process. Technol.* **2014**, *124*, 243–248. [CrossRef]
20. Kaliyan, N.; Vance Morey, R. Factors affecting strength and durability of densified biomass products. *Biomass Bioenergy* **2009**, *33*, 337–359. [CrossRef]
21. Van Eeckhout, E.M. The mechanisms of strength reduction due to moisture in coal mine shales. *Int. J. Rock Mech. Min. Sci. Geomech. Abstr.* **1976**, *13*, 61–67. [CrossRef]
22. Crundwell, F.; Moats, M.S.; Ramachandran, V.; Robinson, T.G.; Davenport, W.G. *Extractive Metallurgy of Nickel, Cobalt and Platinum Group Metals*; Elsevier: Amsterdam, The Netherlands, 2011.
23. Iljana, M. Iron Ore Pellet Properties Under Simulated Blast Furnace Conditions: Investigation on Reducibility, Swelling and Softening. Doctoral Thesis, Faculty of Technology, University of Oulu, Oulu, Finland, 2017; pp. 1–87.
24. *ISO 4700:2015(E)*; Iron Ore Pellets for Blast Furnace And Direct Reduction Feedstocks—Determination of the Crushing Strength. ISO copyright office: Geneva, Switzerland, 2015.
25. *ISO 3271:2015(E)*; Iron Ores for Blast Furnace and Direct Reduction Feedstocks–Determination of the Tumble and Abrasion Indice. ISO copyright office: Geneva, Switzerland, 2015.
26. *ISO 4695:2021(E)*; Iron Ores for Blast Furnace Feedstocks–Determination of the Reducibility by the Rate of Reduction Index. ISO copyright office: Geneva, Switzerland, 2021.
27. *ISO 8371:2015(E)*; Iron Ores for Blast Furnace Feedstocks—Determination of the Decrepitation Index. ISO copyright office: Geneva, Switzerland, 2015.
28. *ISO 4696-1:2015(E)*; Iron Ores for Blast Furnace Feedstocks—Determination of Low-Temperature Reduction-Disintegration Indices by Static Method—Part 1: Reduction with CO, CO2,H2 and N2. ISO copyright office: Geneva, Switzerland, 2015.
29. Goupy, J.L. *Methods for Experimental Design: Principles and Applications for Physicists and Chemists*; Parkes, C.O., Translator; Elsevier: Amsterdam, The Netherlands, 1993.
30. Antony, J. A systematic methodology for design of experiments. *Design of Experiments for Engineers and Scientists*, 2nd ed. Antony, J., Ed.; Elsevier: Edinburgh, UK, 2014; 33–50.
31. Janwong, A. The Agglomeration of Nickel laterite Ore. Doctoral Thesis, Department of Metallurgical Engineering, University of Utah, Salt Lake City, UT, USA, 2012; pp. 26–34.
32. Lu, X.; Guo, E.; Yuan, Q.; Pan, C.; Liu, M. New method to produce FeNi nuggets from low grade ore by semi-molten reduction. In Proceedings of the Thirteenth International Ferroalloys Congress Efficient Technologies in Ferroalloy Industry, Almaty, Kazakhstan, 9–13 June 2013; pp. 223–228.
33. Gleeson, S.A.; Herrington, R.J.; Durango, J.; Velasquez, C.A.; Koll, G. The mineralogy and geochemistry of the Cerro Matoso S.A. Ni laterite deposit, Montelibano, Colombia. *Econ. Geol.* **2004**, *99*, 1197–1213. [CrossRef]
34. Satyananda, P.; Kumar, A.; Rayasam, V. The effect of particle size on green pellet properties of iron ore fines. *J. Min. Metall. A Min.* **2017**, *53*, 31–41. [CrossRef]
35. Xue, Y.; Zhu, D.; Pan, J.; Guo, Z.; Tian, H.; Li, G.; Huang, Q.; Pan, L.; Huang, X. Significant influence of self-possessed moisture of limonitic nickel laterite on sintering performance and its action mechanism. *J. Iron Steel Res. Int.* **2022**, *29*, 1368–1380. [CrossRef]
36. Goenka, M.; Naik, A. Effect of Size Distribution and Water Content on Properties of Iron ore Pellets. B. Tech Thesis, National Institute of Technology, Rourkela, India, 2013. Available online: http://ethesis.nitrkl.ac.in/4902/ (accessed on 12 November 2024).
37. Murakami, T.; Nishimura, T.; Kasai, E. Lowering reduction temperature of iron ore and carbon composite by using ores with high combined water content. *ISIJ Int.* **2009**, *49*, 1686–1693. [CrossRef]

38. Faria, G.L.; Vianna, N.C.S.; Jannotti, N.; Vieira, C.B.; Da Silva, A.F.G. Decrepitation of Brazilian manganese lump ores. In Proceedings of the Twelfth International Ferroalloys Congress: Sustainable Future, Helsinki, Finland, 6–10 June 2010; pp. 449–456.
39. Lu, L. (Ed.) *Iron Ore: Mineralogy, Processing and Environmental Sustainability*; Woodhead Publishing: Cambridge, UK, 2015.
40. Rojas Arias, N.; Perez Villamil, F.R.; Arango Patermina, H.J. Effect of particle size in the reduction of lateritic Ni ore in a Linder reactor. *Rev. ION* **2018**, *31*, 97–104. [CrossRef]
41. Dalvi, A.; Bacon, W.G.; Osborne, R. The past and the future of nickel laterites. In Proceedings of the PDAC 2004 International Convention, Trade Show and Investors Exchange, Toronto, ON, Canada, 7–10 March 2004; pp. 1–27.
42. Moreira Alves, T.; De Souza Sales, P.C. Barro Alto Preliminary Mine Closure Plan. 2022. Available online: https://brasil.angloamerican.com/~/media/Files/A/Anglo-American-Group-v5/Brazil/sustentabilidade/plano-de-fechamento-de-mina-de-barro-alto-2022.pdf (accessed on 1 November 2023).